

Detection and monitoring of localized matrix metalloproteinase upregulation in a murine model of asthma

Csilla N. Felsen,¹ Elamprakash N. Savariar,¹ Michael Whitney,¹ and Roger Y. Tsien^{1,2}

¹Department of Pharmacology and ²Howard Hughes Medical Institute, University of California at San Diego, La Jolla, California

Submitted 23 December 2013; accepted in final form 1 February 2014

Felsen CN, Savariar EN, Whitney M, Tsien RY. Detection and monitoring of localized matrix metalloproteinase upregulation in a murine model of asthma. *Am J Physiol Lung Cell Mol Physiol* 306: L764–L774, 2014. First published February 7, 2014; doi:10.1152/ajplung.00371.2013.—Extracellular proteases including matrix metalloproteinases (MMPs) are speculated to play a significant role in chronic lung diseases, such as asthma. Although increased protease expression has been correlated with lung pathogenesis, the relationship between localized enzyme activity and disease progression remains poorly understood. We report the application of MMP-2/9 activatable cell-penetrating peptides (ACPPs) and their ratiometric analogs (RACPPs) for in vivo measurement of protease activity and distribution in the lungs of mice that were challenged with the allergen ovalbumin. MMP-2/9 activity was increased greater than twofold in whole, dissected lungs from acutely challenged mice compared with control mice ($P = 1.8 \times 10^{-4}$). This upregulation of MMP-2/9 activity was localized around inflamed airways with 1.6-fold higher protease-dependent ACPP uptake surrounding diseased airways compared with adjacent, pathologically normal lung parenchyma ($P = 0.03$). MMP-2/9 activity detected by ACPP cleavage colocalized with gelatinase activity measured with in situ dye-quenched gelatin. For comparison, neutrophil elastase activity and thrombin activity, detected with elastase- and thrombin-cleavable RACPPs, respectively, were not significantly elevated in acutely allergen-challenged mouse lungs. The results demonstrate that ACPPs, like the MMP-2/9-activated and related ACPPs, allow for real-time detection of protease activity in a murine asthma model, which should improve our understanding of protease activation in asthma disease progression and help elucidate new therapy targets or act as a mechanism for therapeutic drug delivery.

asthma; activatable cell-penetrating peptides; matrix metalloproteinases 2 and 9; extracellular proteases

ASTHMA IS A COMMON CHRONIC LUNG DISEASE characterized by intermittent airway obstruction and inflammation that affects more than 300 million people worldwide (5). In both acute and chronic asthma, proinflammatory cells, including neutrophils, eosinophils, mast cells, and macrophages, infiltrate into the lung tissue (4, 22). These proinflammatory cells are known to secrete a variety of extracellular proteases, including matrix metalloproteinases-2 and 9 (MMP-2/9), whose levels have been correlated with lung pathogenesis in asthma (1, 6, 8, 12, 20, 21, 33). The specific contributions of extracellular proteases to asthma disease progression are not well understood in part because it has been difficult to measure localized protease activity in vivo (31). Evidence for the potential involvement of extracellular proteases in asthma primarily consists of mRNA and protein expression profiling of bronchoalveolar lavage

fluid, biopsy tissue, and postmortem lung tissue (8, 9, 15, 20), which does not necessarily reflect the in vivo activity of these proteases and their contributions to the disease pathogenesis. An additional problem with assays using tissue homogenates is their inherent insensitivity to the balance of the inactive pro-forms and the activated form of each protease. Furthermore, complementary inhibitors, such as tissue inhibitors of metalloproteinases, cannot be accounted for in measurements of the protein or mRNA levels. Although genetic knockouts have demonstrated that a subset of extracellular proteases including MMP-2 and MMP-9 are important in asthma pathogenesis (9, 11, 12, 20, 30, 33), knockouts do not give mechanistic insights into the exact timing, location, and relationship of localized protease activation with pathology. Genetic knockouts can also have confounding secondary effects attributable to developmental changes or differential regulation of related proteases that are not directly caused by the absence of the specific protease.

Protease sensors would be useful tools for studying protease activation and determining whether the activity of a protease correlates with asthma disease progression. The detection and evaluation of the protease activity in asthma could improve the early diagnosis and monitoring of disease severity as well as aid in treatment design. In this report, we use activatable cell-penetrating peptides (ACPPs) to monitor MMP activity in murine models of acute and chronic allergen-induced asthma. ACPPs are synthetic, injectable probes that consist of a polycationic cell-penetrating peptide (CPP) attached via a specific, cleavable linker to a polyanionic peptide. The polyanion inhibits the attachment of the CPP to cells and subsequent endocytic uptake. Cleavage of the linker by proteases that are active within diseased tissue releases the inhibitory polyanion, activating the CPP (2, 24). Because cellular uptake depends on activation by specific proteases, ACPPs highlight in vivo proteolytic activity.

Using MMP-2/9-cleavable ACPPs with the cleavage sequence PLGC(Me)AG, we show that MMP-2/9 are upregulated in the lungs of allergen (ovalbumin, OVA)-challenged mice. Furthermore, the highest MMP-2/9 activity was detected in the areas of inflammation surrounding airways, a major site of tissue remodeling in the progression to chronic asthma. Although there are reports that neutrophil elastase and thrombin levels are elevated in asthma (17, 19, 34, 45), we did not detect increased elastase or thrombin protease activity in a murine model of asthma using ACPPs directed at these enzymes. This validation of the application of ACPP technology to asthma increases our basic understanding of the disease pathogenesis and provides a tool for the preclinical evaluation of novel imaging methods and therapies.

Address for reprint requests and other correspondence: R. Tsien, Howard Hughes Medical Institute, Univ. California San Diego, 9500 Gilman Dr., George Palade 310, La Jolla, CA 92093-0647 (e-mail: rtsien@ucsd.edu).

MATERIALS AND METHODS

Synthesis of peptides. The peptides were synthesized as previously described (41). Briefly, standard solid-phase Fmoc syntheses were used to generate the single fluorophore peptides. For the MMP-2/9-cleavable ACPPs (ACPP1A and ACPP1B), H₂N-e₉-c(SS-*t*Bu)-o-PL-GC(Me)AG-r₉-cCONH₂ (synthesized in house) was reacted with Cy5 Maleimide (GE Healthcare). The lower case letters “e”, “c”, and “r” represent D-amino acids; o- denotes 5-amino-3-oxopentanoyl, a short hydrophilic spacer; C(Me) denotes S-methylcysteine; and the final CONH₂ is the COOH-terminal amide. To deprotect the *tert*-BuSH group, the peptide was then treated with triethylphosphine before purification with high-performance liquid chromatography (HPLC). For ACPP1A and ACPP1B, the purified compound was reacted with SPDP-peg12-peg2-peg2-cyclo[RGDfK] and SPDP-peg12-peg2-peg2-cyclo[RADfK], respectively. Detailed chemical structures are reported elsewhere (41). For the synthesis of the ratiometric ACPP MMP-RACPP1, ACPP1B was reacted with Cy7mono NHS ester (Cy7-NHS, GE Health Sciences). The final product was purified using C-18 reverse-phase HPLC. A similar synthetic protocol was used to make the uncleavable controls (UC-ACPP2 and UC-RACPP2), wherein the starting material was instead H₂N-e₉-c(SS-*t*Bu)-o-peg6-r₉-cCONH₂. The starting materials for the elastase- and thrombin-cleavable RACPPs (elastase-RACPP3 and thrombin-RACPP4) were H₂N-e₉-c(SS-*t*Bu)-o-RLQLK(Ac)L-r₉-cCONH₂ and H₂N-e₉-cys-(SS-*t*Bu)-o-(Nle)TPRSFL-r₉-cCONH₂, respectively. Analytical HPLC combined with mass spectrometry (HPLC-MS) was used to monitor all reactions. The final compounds, characterized by HPLC-MS, had greater than 95% purity.

Induction of asthma. The mouse model of OVA-induced asthma has previously been described (16). Female C57BL/6 (6–8 wk old) (Tyrc BrdCrHsd, albino, Harlan Sprague Dawley) mice were sensitized by intraperitoneal (i.p.) injection of 50 µg OVA (Sigma-Aldrich) adsorbed to 500 µg aluminum hydroxide (alum, Sigma-Aldrich) in 200 µl PBS administered on *days 0* and *12*. Mice were challenged with 20 µg of intranasal (i.n.) OVA in 50 µl PBS on *days 24*, *26*, and *28* under isoflurane anesthesia and were killed on *day 29* (acutely challenged mice). Age- and sex-matched control mice were sensitized with OVA and alum but received PBS alone (no OVA) for the challenge phase (control mice). Chronic asthma mice received an additional month of biweekly i.n. challenges (1 challenge every 3–4 days for a total of 8 additional challenges in 4 wk) with OVA (20 µg OVA in 50 µl PBS) (chronically challenged mice). The University of California, San Diego Institutional Animal Care and Use Committee approved all animal experimental protocols (protocol no.: S11195) for the experiments included in this study.

Imaging. The Cy5-labeled (MMP-ACPP1A, MMP-ACPP1B, and UC-ACPP2; 10 nmol each) and ratiometric (MMP-RACPP1, UC-RACPP2, elastase-RACPP3, and thrombin-RACPP4; 5 nmol each) ACPPs were administered intravenously (i.v., retroorbital) or i.n., respectively, while mice were under anesthesia with isoflurane. Within 1–2 min of peptide administration, mice were awake and active. For MMP-ACPP1A and B and UC-ACPP2, 6 h after peptide administration, mice were euthanized by isoflurane overdose followed by cervical dislocation. The skin and ribcage were then removed, after which the lungs were inflated with a mix of Tissue-Tek optimized cooling temperature (OCT) compound (Sakura) and PBS (3:2) and isolated for imaging with a whole body mouse imager (Maestro, CRI). The lungs were imaged with the following settings: excitation of 620/20 nm, emission of 670/10 nm, and exposure time of 1.5 s. For the RACPPs, the same procedure was followed, except the lungs were imaged 2 h after peptide administration. Also, the lungs were imaged immediately after the overlying skin and ribcage were removed, while they were still contained within the mouse (referred to as intact lungs), and were then reimaged after inflation (with OCT and PBS) and removal (referred to as inflated lungs). For in vivo ratiometric imaging, mice were anesthetized with 100 mg/ml ketamine and 10 mg/ml

xylazine, administered i.p.; anesthetic induction was confirmed by loss of the pedal withdrawal reflex, after which animals were given lidocaine near the midline, to minimize pain from the incision, and placed on a Delta-phase isothermal pad to maintain body temperature. Direct-view imaging was achieved after an arc-shaped incision was made in the skin covering the chest wall and a skin flap was reflected away from the mouse, allowing for imaging of the lungs through the ribcage. Ratiometric imaging with the RACPPs was carried out as previously described (41). Briefly, Cy5 was excited at 620/20 nm, and the emission intensity was measured from 640 to 840 nm with a 10-nm step size through a tunable liquid crystal emission filter. The numerator (Cy5) and denominator (Cy7) images were generated by integrating the spectral images at 10-nm intervals over the ranges of 660–720 nm for Cy5 and 760–830 nm for Cy7. Ratiometric images were produced with custom software by dividing the Cy5 emission by the Cy7 emission and creating a pseudocolor for the ratio value from blue (lowest ratio) to red (highest ratio). The brightness for each pixel was based on the corresponding brightness in the original Cy5 image. Regions of interest (~930–1,400 nm²) were delineated and analyzed for the average fluorescence signal or lung ratio using ImageJ.

Histology. Dissected lungs were immediately embedded in Tissue-Tek OCT and frozen. Cryostat sections (10 µm) were obtained and either 1) dried before imaging the Cy5 fluorescence (excitation 635 nm, emission 650 LP) on a confocal microscope (5Live, Zeiss LSM) for MMP-ACPP1A and B and UC-ACPP2 or 2) mounted with PBS to image the Cy5/Cy7 emission ratio (Cy5: excitation 609/54 nm, emission 685/40 nm; Cy7: excitation 609/54 nm, emission 785/62 nm) with a Zeiss epifluorescence microscope for the RACPPs. The same slides that were imaged for the MMP-ACPP1A and B and UC-ACPP2 Cy5 fluorescence were then stained with hematoxylin and eosin (H&E) for histological analysis and imaged using a Nanozoomer 2.0HT (Hamamatsu). ImageJ was used to measure the fluorescence intensity and ratios for the ACPPs and RACPPs, respectively. First, the threshold was adjusted to only include the lung tissue, excluding the blank air spaces. Then, the mean fluorescence intensity (MFI) or ratio was measured for the entire image, including the tissue surrounding the airways and the lung parenchyma. To compare the ACPP signal surrounding inflamed airways vs. in the lung parenchyma, comparable regions of interest (483 µm²) were separately drawn around the inflamed airway vs. in the lung parenchyma before the intensity was measured for each.

In situ zymography. Gelatinolytic activity was examined in unfixed cryostat sections (10 µm) using dye-quenched (DQ) gelatin as a substrate (Enz-Chek, Molecular Probes). Lung sections from acutely challenged and control mice that were previously injected in vivo with MMP-ACPP1B and UC-ACPP2 were air dried for 10 min and washed once with PBS to remove the OCT. DQ gelatin was dissolved to 1 mg/ml in nanopure water and then diluted 1:10 in 1% (wt/vol) low gelling temperature agarose (Sigma) in PBS. The DQ gelatin mixture (40 µl) was added to the lung sections, and the slides were covered with coverslips. After the agar was gelled at 4°C, incubation was performed for 1 h at room temperature before imaging with a Zeiss LSM 5Live microscope (Hoechst nuclear stain: excitation 405/emission 415–480 nm; DQ gelatin FITC: excitation 488/emission 500–525 nm; and Cy5 ACPP signal: excitation 635/emission 650 LP nm). The MMP-2/9-independent DQ gelatin background signal was determined with 1 mM 1,10-phenanthroline (Sigma-Aldrich) (29), a zinc chelator, which was added to the DQ gelatin and agarose mixture for simultaneous incubation with the lung sections. To evaluate autofluorescence, DQ gelatin alone (no tissue) and lung tissue in the absence of DQ gelatin were also imaged at matched settings; the background was not significant.

Statistical analyses. Statistical analyses were conducted using the two-tailed Student's *t*-test, and all results are given as the means ± standard deviation. *P* < 0.05 was considered statistically significant.

RESULTS

Evaluating MMP-2/9 activity in murine asthma with single fluorophore ACPPs. To detect MMP-2/9 activation in a murine model of asthma, we monitored the cleavage and accumulation of MMP-2/9-cleavable ACPPs in the lungs of mice that were acutely challenged with OVA allergen (acutely challenged mice) and compared the uptake with lungs from control mice that were only sensitized to OVA (control mice). In addition to having an MMP-2/9-cleavable linker, PLGC(Me)AG, our ACPPs were also linked to either a cyclic-RGD (MMP-ACPP1A) or cyclic-RAD (MMP-ACPP1B) peptide through a peg12 linker adjacent to the protease activation site. The aim of this design was to preconcentrate MMP-ACPP1A near MMP-2 because of the affinity of cyclic(RGD) to integrin $\alpha_v\beta_3$ and the reported interaction of the MMP-2 hemopexin domain with integrin $\alpha_v\beta_3$ (7). Although there are no reports of $\alpha_v\beta_3$ upregulation in murine asthma, activated macrophages, like those present in murine asthma, are reported to have high integrin $\alpha_v\beta_3$ activity (3). Expression of integrin $\alpha_v\beta_3$ has also been reported in the alveolar endothelium, vascular smooth muscle, and bronchial epithelium (43).

To test for ACPP uptake, mice were intravenously injected with 10 nmol of Cy5-labeled MMP-ACPP1A, MMP-ACPP1B, or uncleavable control ACPP (UC-ACPP2), which has a protease-resistant peg6 linker in place of PLGC(Me)AG. After 6 h, mice were euthanized, and their lungs were removed and immediately imaged using identical capture settings. Uptake, as determined by the MFI, of MMP-ACPP1B was twofold higher in lungs from acutely challenged mice than control mice (acutely challenged MFI = $1,028.6 \pm 156.4$ vs. control MFI = 503.0 ± 87.7 , $n = 5$ each, $P = 1.8 \times 10^{-4}$; Fig. 1, C–E). The uptake of MMP-ACPP1A in acutely challenged mice trended higher than MMP-ACPP1B, but this difference was not significant (1.3-fold higher; $P = 0.06$), indicating that conjugation of cyclic(RGD) to the ACPP did not have a significant effect on in vivo targeting in this model. This may indicate that cleavage of MMP-2/9-cleavable ACPP in this model may be more dependent on MMP-9 or other related MMPs that do not directly interact with integrin $\alpha_v\beta_3$ or that the cyclic(RGD) on MMP-ACPP1A is instead inhibiting integrin $\alpha_v\beta_3$. MMP-

ACPP1B uptake was 1.9-fold higher than UC-ACPP2 in lungs from acutely challenged mice (MFI UC-ACPP2 = 551.9 ± 142.3 , $n = 5$, $P = 0.001$; Fig. 1, B and E).

Although there was significantly higher uptake of MMP-ACPP1B compared with UC-ACPP2 in acutely challenged lungs, UC-ACPP2 still had higher uptake in lungs from acutely challenged mice than in control mice. This uptake may be due to binding of UC-ACPP2 to proteoglycans in acutely challenged lungs. We have previously seen significant, nonspecific uptake of ACPPs in proteoglycan-rich cartilage and areas of increased inflammation although this nonspecific uptake can be almost completely eliminated by attachment of ACPPs to high molecular weight carriers (36). Supporting this hypothesis, there have been reports that negatively charged proteoglycans are increased in murine models of OVA-induced asthma (32) and in patients with asthma (28, 40).

To further analyze the protease-dependent uptake of the MMP-2/9-cleavable ACPPs, lung tissue from mice that had been previously injected with ACPPs was sectioned and imaged using confocal microscopy. To measure the MFI of lung sections, the threshold was adjusted in ImageJ to only include the lung tissue, excluding the blank air spaces; then, the MFI was measured for the entire lung section. Additionally, the MFI in equal-sized regions of interest of 1) the areas surrounding airways and 2) the normal lung parenchyma were separately measured to compare the uptake around inflamed airways with the adjacent lung tissue. Again, ACPP cleavage and uptake were significantly higher in lungs from acutely challenged mice that had been previously injected with MMP-ACPP1B (MFI = $12,297.4 \pm 1,736.4$; Fig. 2, D and I) than in mice injected with UC-ACPP2 (MFI = $6,175.9 \pm 627.2$, $P = 4.6 \times 10^{-3}$; Fig. 2, B and I) as well as in control mice that were injected with MMP-ACPP1B (MFI = $6,904.5 \pm 283.2$, $P = 6.0 \times 10^{-3}$; Fig. 2, C and I). These results were comparable with the whole lung imaging results, confirming protease-dependent uptake of the MMP-2/9-cleavable ACPP in lungs from acutely challenged mice. Lung tissue from these mice was then analyzed histologically by H&E staining (Fig. 2, E–H). The areas surrounding the airways of acutely challenged mice were dense with infiltrating inflammatory cells, a feature

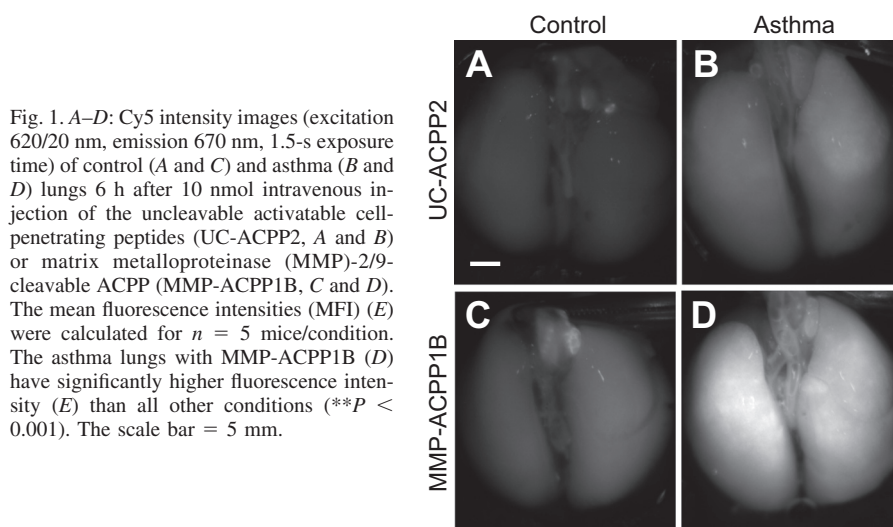
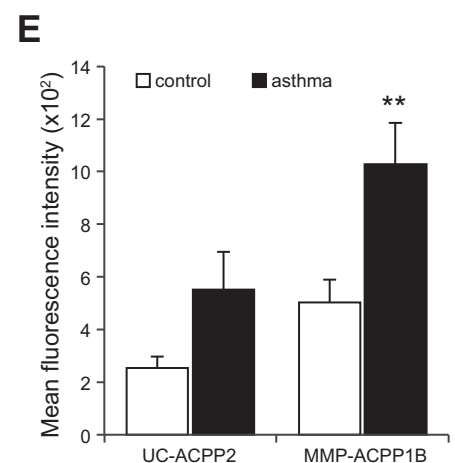


Fig. 1. A–D: Cy5 intensity images (excitation 620/20 nm, emission 670 nm, 1.5-s exposure time) of control (A and C) and asthma (B and D) lungs 6 h after 10 nmol intravenous injection of the uncleavable activatable cell-penetrating peptides (UC-ACPP2, A and B) or matrix metalloproteinase (MMP)-2/9-cleavable ACPP (MMP-ACPP1B, C and D). The mean fluorescence intensities (MFI) (E) were calculated for $n = 5$ mice/condition. The asthma lungs with MMP-ACPP1B (D) have significantly higher fluorescence intensity (E) than all other conditions (** $P < 0.001$). The scale bar = 5 mm.



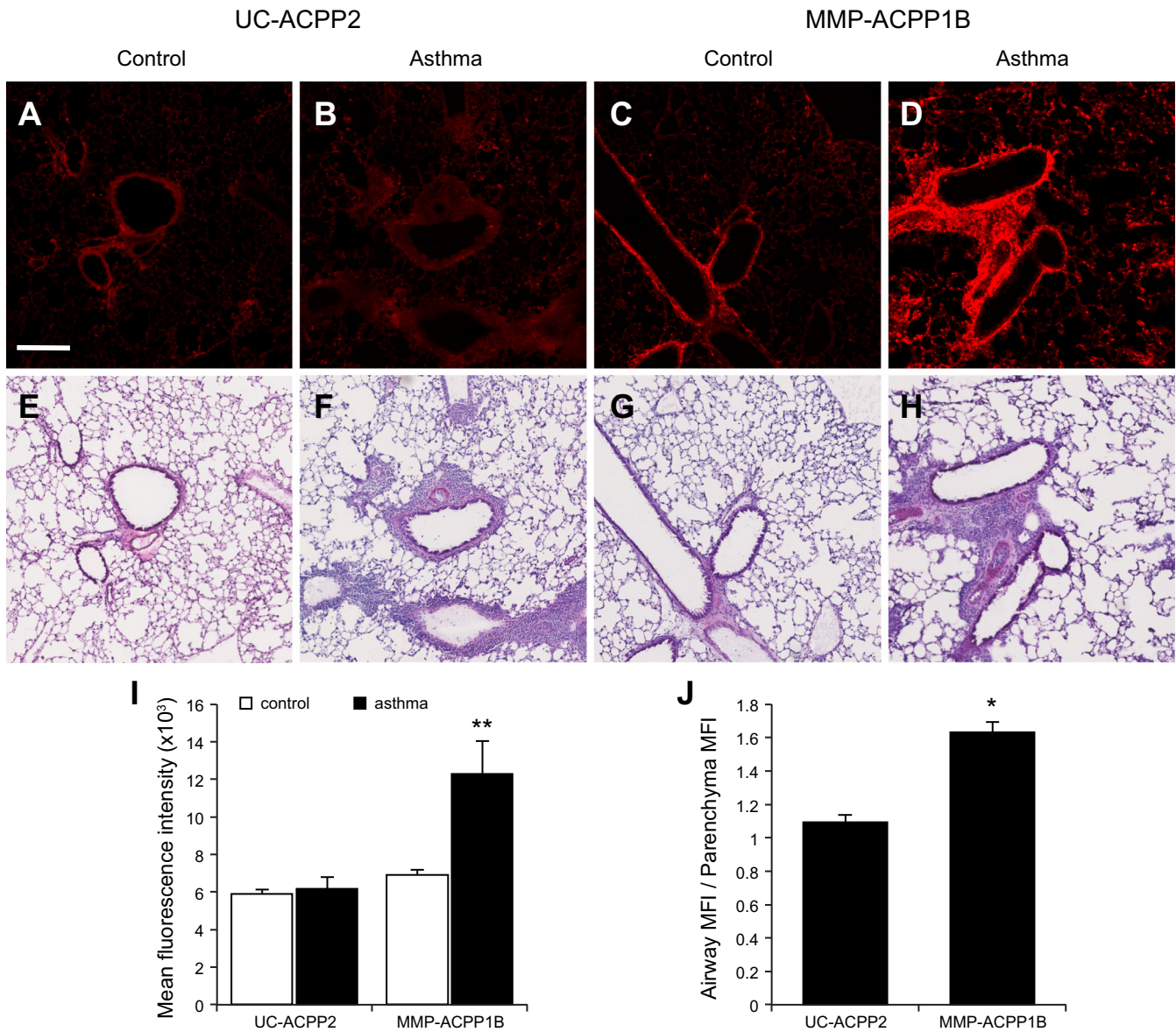


Fig. 2. *A–D*: fluorescence images of acute asthma and control lung sections (10 μ m) corresponding to the mice in Fig. 1. With the UC-ACPP2, the control (*A*) and asthma (*B*) lungs have low fluorescence signal. Whereas the control lungs maintain low signal with the MMP-ACPP1B (*C*), the asthma lungs with MMP-ACPP1B (*D*) have higher signal than all other conditions. *E–H*: corresponding hematoxylin and eosin-stained sections for the fluorescent images in *A–D*. Images were acquired by confocal imaging of 4×4 tiles and are representative samples from a set of 8 images per mouse for $n = 3$ mice/condition. The scale bar = 200 μ m. The MFI (*I*) and the ratio of the airway MFI to parenchyma MFI (*J*) were calculated for all acquired images (* $P < 0.05$; ** $P < 0.001$).

that has been previously reported in a comparable mouse model of asthma (39). The highest localized probe uptake was in the regions surrounding the airways in lungs from the acutely challenged mice that had been injected with MMP-ACPP1B (Fig. 2*D*). MMP protease-dependent Cy5 fluorescence was 1.6-fold higher around these inflamed airways compared with adjacent, pathologically normal lung parenchyma ($P = 0.03$; Fig. 2*J*). In comparison, the Cy5 fluorescence of surrounding airways was similar to the parenchyma from acutely challenged mice that had been injected with UC-ACPP2 (Fig. 2*B*), and the ratio of the airway signal to parenchyma was 1.1 ($P = 2.1 \times 10^{-4}$; Fig. 2*J*).

Colocalization of MMP-ACPP1B with *in situ* DQ gelatinase activity. To confirm that MMP-ACPP1B uptake correlates with MMP-2/9 gelatinase activity, we compared the microscopic

localization of MMP-ACPP1B uptake with a commonly used method for detecting MMP-2/9 activity in tissue sections, *in situ* DQ gelatin. We treated 10- μ m lung sections from mice that were injected *in vivo* with either MMP-ACPP1B or UC-ACPP2 with DQ gelatin for *in situ* detection of gelatinase activity. Lungs from acutely challenged mice that had been injected with MMP-ACPP1B had high Cy5 fluorescence signal from the cleaved ACPP (Fig. 3*J*) and high MMP-2/9 activity, visible by dequenching of the DQ gelatin substrate (Fig. 3*J*), that colocalized to areas of inflammation surrounding the airways (see yellow area, Fig. 3*K*). For comparison, lungs from control mice that had been previously injected with MMP-ACPP1B had low signal from both DQ gelatin (Fig. 3*A*) and the ACPP (Fig. 3*B*). Lungs from acutely challenged mice that had been previously injected with control UC-ACPP2 had low

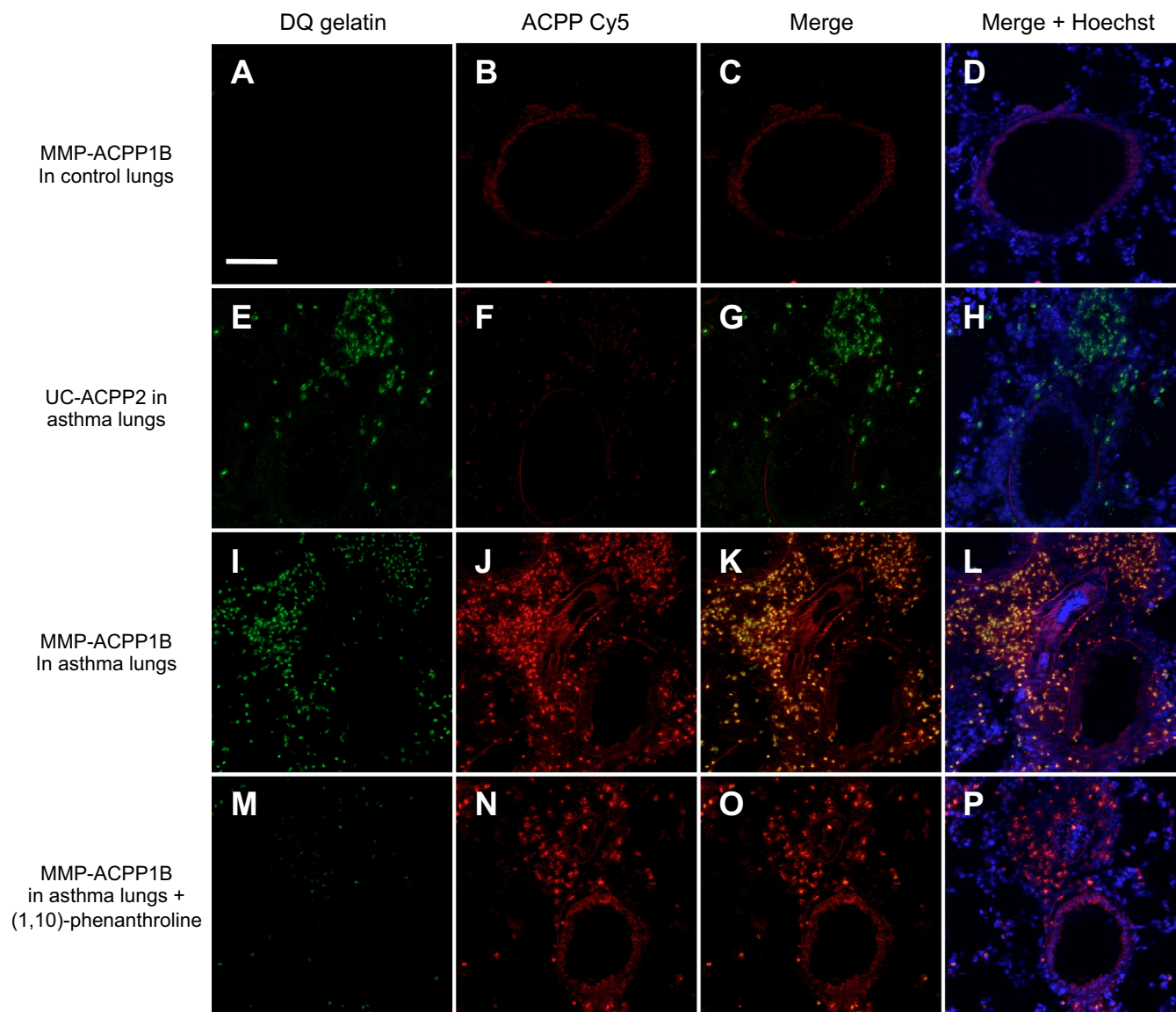


Fig. 3. Fluorescence images of acute asthma and control lung sections (10 μm thick) that were treated with dye-quenched (DQ) gelatin after in vivo injection of cleavable and uncleavable ACPPs. For the control lungs with the MMP-ACPP1B, (A–D), there is low signal from both the DQ gelatin (A) and ACPP (B) at these imaging settings. For the asthma lungs with the UC-ACPP2 (E–H), there is low signal from the ACPP (F) with substantial signal from the DQ gelatin (E). For MMP-ACPP1B in asthma lungs (I–L), there is high signal in from both the DQ gelatin (I) and ACPP (J) that has substantial overlap in an overlay of the two (K and L); the DQ gelatin signal is significantly decreased when the slide is cotreated with 1,10-phenanthroline (M), with not much of an effect on the ACPP signal (N–P) because uptake is completed in vivo. The scale bar = 400 μm .

Cy5 ACPP signal (Fig. 3F) but high DQ gelatin signal (Fig. 3E). Thus neither control condition had colocalization between the ACPP and DQ gelatin fluorescence signal (Fig. 3, C and G, respectively). The DQ gelatin signal was substantially knocked down by the addition of 1 mM 1,10-phenanthroline, a broad-spectrum MMP inhibitor (Fig. 3M). The MMP inhibitor did not affect the ACPP uptake (Fig. 3N) because the lungs were harvested from animals that had been previously injected with MMP-ACPP1B, and uptake occurred before the addition of the inhibitor. These results demonstrate that there was in vivo activation and uptake of MMP-ACPP1B in localized regions of MMP-2/9 activity, as confirmed ex vivo with DQ gelatin.

Evaluating MMP-2/9 activity in asthma with a RACPP. To further investigate MMP-2/9 activity in the murine model of OVA-induced asthma, we also tested a ratiometric MMP-2/9-

cleavable ACPP (MMP-RACPP1). RACPPs have previously been described for use in cancer and allow for real-time monitoring of cleavage without requiring probe washout (41). Unlike single fluorophore ACPPs, RACPPs have a Cy7 acceptor fluorophore attached to the COOH terminus of the polycationic inhibitory domain. In the intact RACPP, Cy5 (excitation max \sim 630 nm; emission max \sim 670 nm) and Cy7 (excitation max \sim 700 nm; emission max \sim 780 nm) are in close proximity and undergo fluorescence resonance energy transfer (FRET). When MMP-2/9 cleave the linker, the resulting separation of the polyanionic and polycationic sequences disrupts the FRET, allowing the adhesive Cy5-labeled CPP to bind and enter cells while instantly restoring the Cy5 intensity and eliminating the Cy7 reemission. Therefore, the ratio of the Cy5 emission/Cy7 emission gradually increases as the RACPP is cleaved. Wash-

out of the uncleaved peptide is not required to observe protease activity because the spectra of the cleavable and uncleavable RACPPs can be differentiated. As a result, imaging can be initiated immediately after the administration of RACPP, and RACPPs can be more selectively directed to lungs via i.n. administration, allowing for real-time detection of MMP activity through *in vivo* monitoring of the Cy5-to-Cy7 (Cy5/Cy7) emission ratio.

To test for the *in vivo* cleavage of the RACPP, mice were i.n. administered RACPP (5 nmol) followed by partial dissection to expose the lungs for imaging 2 h after injection of the probe. The lower (5 nmol) i.n. dose compared with i.v. administration of the single fluorophore ACPPs was selected after a pilot test with 2.5–10 nmol. The lung ratios were the same for 2.5, 5, and 10 nmol, but we achieved optimal signal detection with our imaging system at 5 nmol. Lungs from acutely challenged mice that received MMP-RACPP1 had a Cy5/Cy7

emission ratio that was twofold higher than lungs from control mice that also received MMP-RACPP1 (acutely challenged Cy5/Cy7 ratio = 3.3 ± 0.3 and control Cy5/Cy7 ratio = 1.7 ± 0.2 , $P = 9.2 \times 10^{-7}$; Fig. 4B). Protease-dependent cleavage of MMP-RACPP1 was 2.9-fold higher than uncleavable UC-RACPP2 (Cy5/Cy7 ratio = 1.1 ± 0.2 , $P = 9.7 \times 10^{-8}$) in lungs from acutely challenged mice (Fig. 4B). Lungs were then inflated and removed before reimaging (Fig. 4A). The ratio values for the inflated lungs were not significantly different from the intact lungs (challenged lungs with MMP-RACPP1 Cy5/Cy7 ratio = 3.4 ± 0.3 or UC-RACPP2 Cy5/Cy7 ratio = 1.5 ± 0.3 and control lungs with MMP-RACPP1 Cy5/Cy7 ratio = 1.8 ± 0.1). With this alternative route of administration, MMP-2/9-dependent signal was detected at a reduced dose (5 nmol vs. 10 nmol) and after a shorter incubation time (2 h vs. 6 h). To verify that postmortem detection of MMP-2/9 activity in intact and inflated and removed lungs was consistent

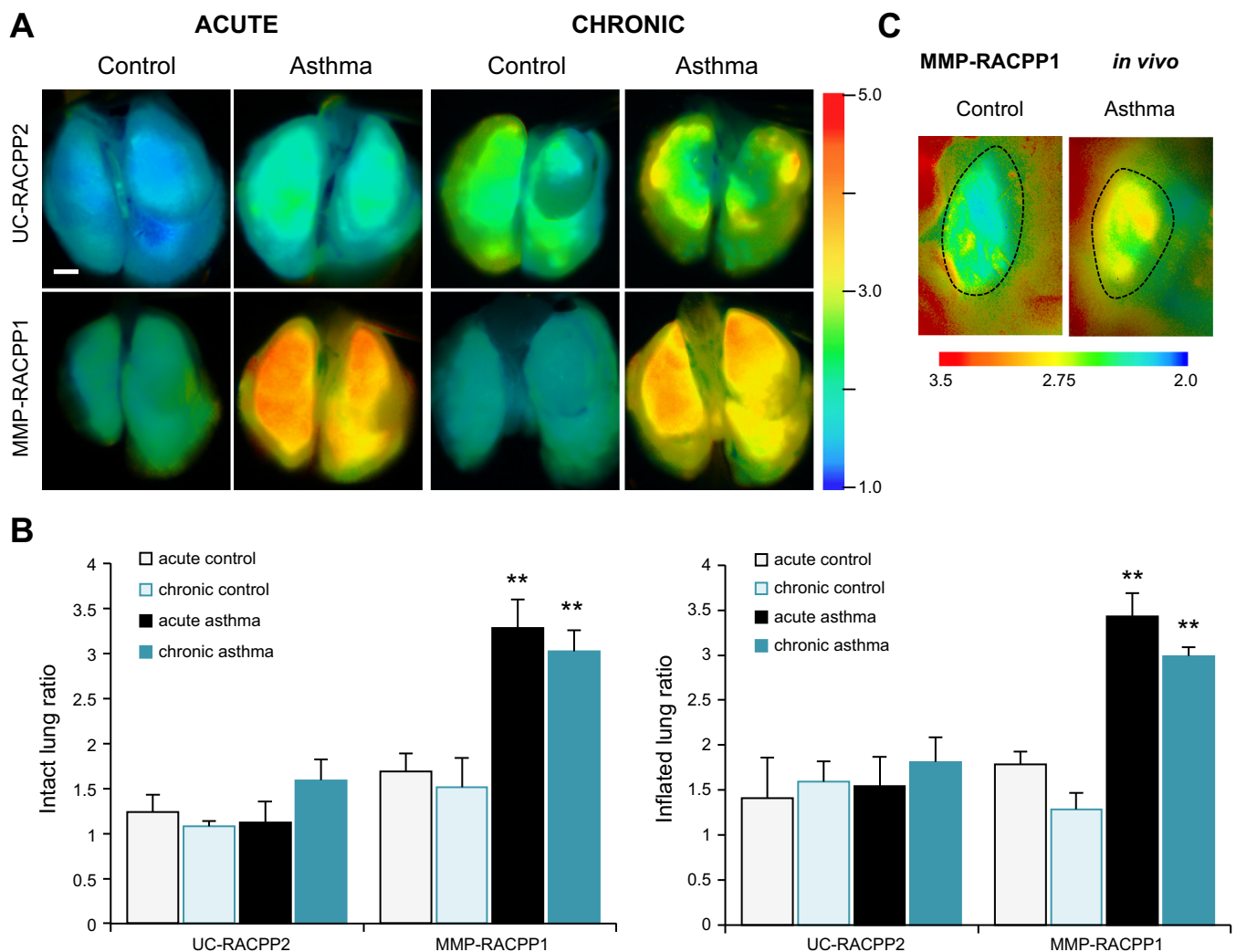


Fig. 4. A: ratiometric imaging of extracted and inflated [optimized cooling temperature compound (OCT) and PBS, 3:2 ratio] lungs 2 h after intranasal administration of ratiometric analogues of ACPPs (RACPPs) (5 nmol). With the UC-RACPP2, the control and asthma lungs have a low ratio. Whereas the control lungs maintain a low ratio with the MMP-RACPP1, the acute and chronic asthma lungs with MMP-RACPP1 have significantly higher ratios (** $P < 0.001$) than all other conditions, as quantified for the intact lungs from 2 independent experiments of $n = 3$ mice/condition each (acute) or a single experiment of $n = 4$ mice/condition (chronic) (B). The scale bar = 5 mm. C: *in vivo* ratiometric imaging of MMP-RACPP1 in control and asthma lungs; a single lung lobe is shown for each image. Before the imaging, a skin flap was removed for visualization of the lungs through the intact ribcage. All asthma lungs had higher ratios than all control lungs. Dashed lines indicate the lung outlines as determined by comparison with the Cy5 fluorescence images.

with the levels in live animals, we imaged a small subset of mice that were kept under deep anesthesia during imaging. In these animals, the lungs were partially exposed by removing a skin flap over the ribcage for live animal imaging through the ribcage. As predicted, the MMP-RACPP1 Cy5/Cy7 emission ratio was higher in the lungs of acutely challenged mice compared with control mice ($n = 3$ for each; $P = 0.01$) (Fig. 4C).

In addition to testing for MMP-2/9 upregulation in the lungs of acutely OVA-challenged mice, we investigated whether increased MMP-2/9 upregulation was detectable in the lungs of mice that underwent a chronic challenge with OVA. Chronic allergen challenge was similar to acute challenge, with i.p. OVA sensitization and i.n. OVA challenge, followed by an additional month of biweekly i.n. challenges (total of 8). The Cy5/Cy7 emission ratios for surgically exposed lungs from chronically challenged mice that had been treated with MMP-RACPP1 were twofold higher than the lungs from age-matched, control mice (chronically challenged Cy5/Cy7 ratio = 3.0 ± 0.2 , control Cy5/Cy7 ratio = 1.5 ± 0.3 , $n = 4$ each, $P = 3.0 \times 10^{-4}$; Fig. 4). Thus MMP activity is upregulated during both the early and later stages of potential asthma progression after challenge with lung allergens.

The results from whole lung imaging with MMP-RACPP1 and UC-RACPP2 in acutely challenged and control mice were validated microscopically with epifluorescence imaging of 10- μm sections from the mice described in Fig. 4 (Fig. 5). Lungs from acutely challenged mice had the highest localized MMP-2/9 activity with a Cy5/Cy7 ratio for MMP-RACPP1 of 3.4 ± 0.7 (Fig. 5, D and E). Lungs from control mice that received MMP-RACPP1 had some bright spots with high ratios, but, overall, the Cy5/Cy7 ratios were 2.2-fold lower than the acutely challenged mice (1.6 ± 0.1 , $P = 0.01$; Fig. 5C). The lowest Cy5/Cy7 ratios, indicating little to no MMP-2/9 cleavage, were observed in the lungs from control and acutely challenged mice treated with UC-RACPP2 (control Cy5/Cy7 ratio = 1.3 ± 0.1 , acutely challenged Cy5/Cy7 ratio = 1.3 ± 0.2 ; Fig. 5, A and B), which were, respectively, 2.5- and 2.6-fold lower than the lungs from acutely challenged mice that received MMP-RACPP1 ($P = 7.5 \times 10^{-3}$ and $P = 6.9 \times 10^{-3}$, respectively).

Evaluating protease activity with RACPPs for a variety of substrates. To evaluate whether other extracellular proteases are upregulated in the lungs of acutely challenged mice, we used RACPPs that are selective for neutrophil elastase (41, 46) and thrombin (47), which were generated by modifying the cleavable linker to alter the substrate specificity (Fig. 6). It has previously been shown that elastase levels are elevated in the sputum of patients with asthma (17) and that neutrophils from patients with asthma release elastase when challenged with allergen (34). Thus we expected that elastase activity would be upregulated in lungs from acutely challenged mice. For the elastase-cleavable RACPP, elastase-RACPP3, there was a trend toward higher elastase activity in the lungs of acutely challenged mice (acutely challenged Cy5/Cy7 ratio = 2.1 ± 0.3 , control Cy5/Cy7 ratio = 1.5 ± 0.4 , $n = 3$ mice each), but the increase was not significant ($P = 0.10$; Fig. 6, A and B) and was even less significant in chronically challenged mice ($P = 0.21$, $n = 4$ mice each, data not shown). Additionally, airway inflammation can cause leakage of plasma proteins, such as thrombin, onto the airway surface, and there are higher levels of extravascular thrombin in the sputum from patients with asthma than control subjects (19, 45). However, as for elastase-RACPP3, the thrombin-cleavable RACPP, thrombin-RACPP4, did not have higher activity in acutely challenged mice compared with control mice (acutely challenged Cy5/Cy7 ratio = 2.7 ± 0.3 , control ratio = 4.0 ± 0.5 , $n = 5$ mice each; Fig. 6, A and B).

DISCUSSION

ACPPs have proven valuable in the detection of protease activity in cancer (2, 24, 35–37, 46) and atherosclerosis (38). More recently, the development of ratiometric ACPPs has improved cancer detection (41) and allowed for in vivo assessment of thrombin activation (47). However, the usefulness of ACPPs has not previously been evaluated in allergic airway inflammation or asthma.

In this study, we demonstrate that both single-fluorophore ACPPs and RACPPs report at least twofold higher MMP-2/9 activity in a model of OVA-challenged asthma compared with control lungs with i.v. (6 h incubation) and i.n. administration

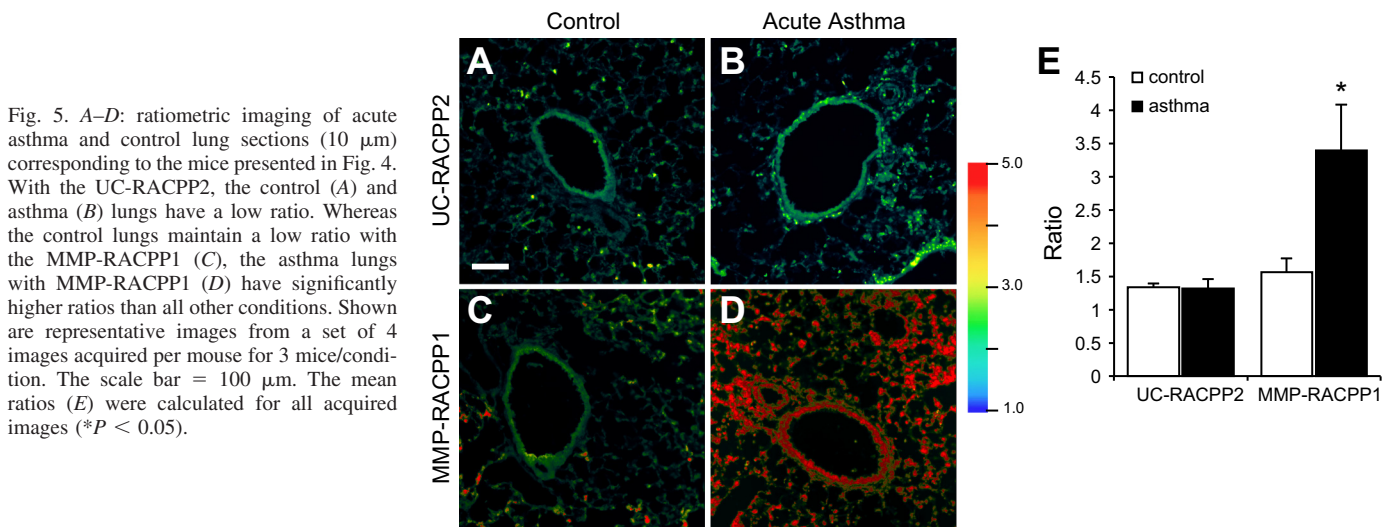


Fig. 5. A–D: ratiometric imaging of acute asthma and control lung sections (10 μm) corresponding to the mice presented in Fig. 4. With the UC-RACPP2, the control (A) and asthma (B) lungs have a low ratio. Whereas the control lungs maintain a low ratio with the MMP-RACPP1 (C), the asthma lungs with MMP-RACPP1 (D) have significantly higher ratios than all other conditions. Shown are representative images from a set of 4 images acquired per mouse for 3 mice/condition. The scale bar = 100 μm . The mean ratios (E) were calculated for all acquired images (* $P < 0.05$).

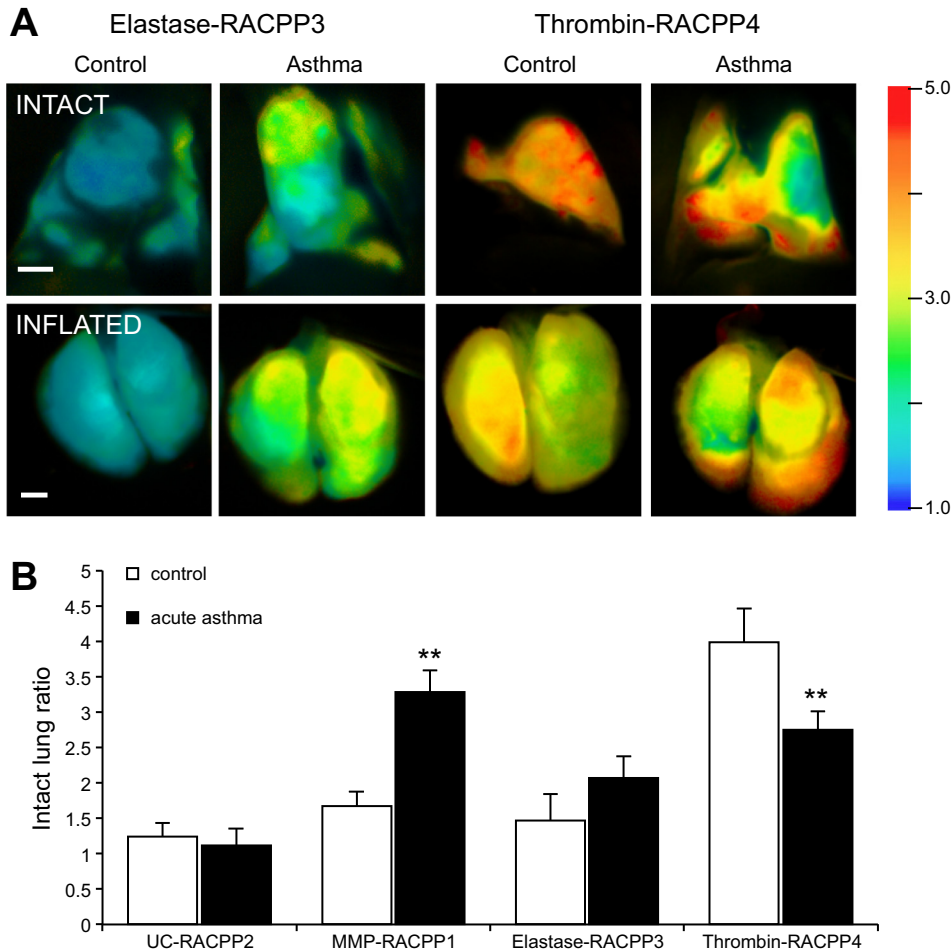


Fig. 6. Ratiometric imaging of intact lungs (A, top) contained within the whole mouse, with the overlying skin and ribcage removed, and extracted and inflated (OCT and PBS, 3:2 ratio) lungs (A, bottom) 2 h after intranasal administration of RACPPs (5 nmol). The elastase-cleavable RACPP (elastase-RACPP3, $n = 3$ mice/condition) had a trend toward higher ratios in asthma than in control lungs, which was not significant ($P > 0.05$). The thrombin-cleavable RACPP (thrombin-RACPP4, $n = 5$ mice/condition) did not have higher ratios in asthma than control lungs. The scale bar = 5 mm. B: summary of the intact lung ratios for all RACPPs tested. All cleavable RACPPs in asthma had higher ratios than the uncleavable RACPP, but only MMP-2/9 had significantly higher activity in asthma than in controls (** $P < 0.001$).

(2 h incubation), respectively. Our findings on the elevated levels of MMP-2/9 in murine asthma are in agreement with studies by Kumagai et al. (27) and Kim et al. (26) reporting higher MMP-2/9 levels in bronchoalveolar lavage fluid from an OVA-induced murine asthma model, which was also approximately twofold higher than control samples according to zymography in the latter study. We observed elevated MMP-2/9 activity in acutely and chronically challenged mice (1-mo additional challenge) with *in vivo* and *ex vivo* analysis of MMP-2/9-cleavable ACPPs in murine lungs. With microscopic imaging of lung sections, the highest accumulation of ACPPs was in the areas of inflammation surrounding asthmatic airways. After the inflammatory cells internalize the ACPP, they may be expected to move beyond the original site of MMP-2/9 activity. However, as visible in Fig. 3, I and J, most of the punctate fluorescence signals from ACPP and DQ gelatin colocalize to the same cells, suggesting negligible migration of these cells from the original sites of MMP-2/9 activity. Additionally, the ACPPs will be taken up in higher levels by the cells that originally released the MMPs compared with nearby cells, allowing us to image the inflammatory cells with the highest MMP-2/9 activity that thus promote airway inflammation in asthma. The ACPP accumulation was significantly lower in the unaffected parenchyma. The higher signal surrounding the airway compared with the parenchyma is expected given that one of the principal differences between

allergen-challenged and control lungs is the recruitment of inflammatory cells in the former, such as neutrophils and eosinophils, which are known to secrete MMP-9 (14, 18, 42, 44) and likely other proteases. Also, in the OVA model of asthma, the parenchyma is unaffected by challenges with OVA (39).

Previous studies have demonstrated a correlation between MMP-2/9 levels and increased lung pathogenesis in asthma (8, 21, 33). However, unlike *ex vivo* tissue analyses of mRNA or protein expression levels, which do not consider the balance of proteases and their inhibitors, ACPPs are uniquely designed to directly detect *in vivo* protease activity because their uptake depends on cleavage by the target protease (MMP-2/9 in this case). Cortez-Retamozo et al. (13) also reported higher MMP activity from a pan-MMP sensor in acutely challenged mice compared with control mice, which they mostly attributed to MMP-12 activity. However, this is the first report to validate that the higher *in vivo* MMP-2/9 protease activity in acutely challenged murine lungs corresponds to areas of higher inflammation surrounding the airways via microscopic imaging of lung sections. Whereas Cortez-Retamozo et al. (13) validated their *in vivo* findings by investigating the MMP activity of individual cells, we assessed the *in vivo* MMP-2/9-cleavable ACPP products in lung sections and found colocalization with MMP-2/9 activity assessed by an alternative method, DQ gelatin *in situ* zymography. This colocalization also means that

the CPP does not travel more than a few tens of microns after cleavage. Given that the cleavable, but not the uncleavable, ACPP colocalized with DQ gelatin, ACPPs are at least as sensitive as DQ gelatin in imaging MMP-2/9 activity with the additional benefit that they can be used for assessing *in vivo* activity. Additionally, not only did we see increased MMP-2/9 activity in acutely challenged lungs, elevated MMP-2/9 activity was maintained throughout the early stages of airway remodeling, as seen with the high MMP-2/9 activity in chronically challenged mice. Although there are reports of increased MMP-9 levels in patients with asthma who undergo antigen challenge (25), there are no current reports on the maintenance of MMP-2/9 activity throughout chronic airway remodeling.

A beneficial feature of the ACPP design is that the linker sequence can easily be replaced with a substrate for any other extracellular protease that has a known cleavage sequence; the chemical approaches for the cleavage sequences reported in this paper have all been previously published (10, 24, 41, 46, 47). Thus ACPPs can be used to examine other extracellular proteases that have proposed activity in asthma. Although we tested RACPPs with substrate sequences specific to elastase and thrombin, neither was as effective as MMP-2/9 at differentiating between high protease activity in acutely challenged vs. control lungs. Although it was unexpected that elastase and thrombin, which have reportedly increased expression levels in asthma, do not have higher activity in acutely challenged vs. control lungs, these negative results help validate the specificity of the MMP-2/9-cleavable ACPP as an *in vivo* reporter of MMP-2/9 activity. Furthermore, although thrombin and elastase mRNA and protein levels may be elevated in asthma, lower levels of translation and processing or the presence of complementary inhibitors could knock down their activity. If the *in vivo* activity of an extracellular protease is not higher in allergen-challenged lungs than in controls, the protease is unlikely to contribute to the disease progression.

The imaging probes used by Cortez-Retamozo et al. (13) rely on separation of the fluorophores, limiting them to fluorescence imaging with no mechanism for retention at the site of cleavage. By contrast, ACPP-targeted cargos accumulate at the site of protease activity, and ACPPs have been applied to nonoptical magnetic resonance imaging (MRI) by replacing the Cy5 with gadolinium for cancer imaging (37). Noninvasive asthma imaging is important because bronchial biopsies taken from large proximal airways are not always representative of the overall disease remodeling (23). Also, by not relying on fluorescence dequenching as our main mechanism of activation or visualization of protease activity, we were able to develop an RACPP. The RACPP allows us to directly assess MMP-2/9 cleavage activity through the ratio of the Cy5 emission (cleaved probe)/Cy7 emission (uncleaved probe). The RACPP ratiometric signal is superior to single fluorophore signal because it does not depend on many nonenzymatic factors that can otherwise perturb single wavelength intensity measurements, such as the illumination intensity, detection sensitivity, and probe concentration. Additionally, unlike for the nonratiometric, single-fluorophore ACPP, washout of the uncleaved probe is not necessary for the RACPP to produce contrast. Finally, the ACPP design allows for the Cy5 cargo to be potentially replaced with a drug that could be targeted to regions of high inflammation and long-term structural damage that contribute to asthma disease progression.

A limitation of this study is our lack of definitive proof that the MMP-2/9-cleavable ACPPs are exquisitely specific for MMP-2/9 activity in this model of asthma. Previous studies in cancer demonstrate specificity of PLGC(Me)AG cleavage by showing lack of cleavage and uptake in MMP-2/9 double-knockout mice that lacked MMP-2/9 activity. A potential complication for using the MMP-2/9 double-knockout mice in asthma is that OVA challenge has been reported to increase inflammation compared with wild-type mice (11). This would be expected to increase protease-independent uptake of ACPPs and could lead to compensatory expression of other MMPs that have similar substrate preferences as MMP-2 and MMP-9 (41). However, the *in situ* DQ gelatin analysis that we present is an orthogonal method for specifically assessing MMP-2/9 activity. The colocalization of the MMP-2/9 activity from the DQ gelatin with that of the *in vivo* incubated ACPPs makes a strong case for the role of MMP-2/9 in the cleavage and activation of our ACPPs in this murine asthma model.

In summary, with the help of activatable peptides that demonstrate extracellular protease activity instead of expression levels, we have demonstrated that MMP-2/9 activity is upregulated in a murine model of acute asthma, and elevated activity is maintained through the early stages of chronic airway remodeling. ACPPs have potential application for clinical diagnosis even before the onset of asthma symptoms or attacks. Although the immediate application of the current fluorescence-based ACPP design to clinical use would require the use of fiberoptic bronchoscopy to detect asthma in the clinic, which can be applied to image up to the fourth-order bronchi, ACPPs are potentially adaptable to less invasive modalities, such as MRI, that would be more favorable to the already irritable asthma airways. Validation of the use of ACPP technology in asthma increases our understanding of the pathogenesis of asthma and provides a powerful tool for preclinical evaluation of novel imaging techniques and therapies.

ACKNOWLEDGMENTS

The authors thank the members of the Tsien laboratory for helpful discussions and comments on the manuscript and work provided therein; Drs. David Broide and Jae Youn Cho for training in asthma model development; Paul Steinbach, Perla Arcaira, and Jessica Crisp for technical support; and the UCSD School of Medicine Light Microscopy Facility for technical assistance in image acquisition with the Nanozoomer (NS047101).

GRANTS

This work was funded by a training grant (5R25CA153915) and F30 fellowship (1F30HL118998-01) to C. Felsen, an ICMIC NCI-P50-CA128346 career development grant to E. Savariar, and the Howard Hughes Medical Institute as well as a grant from the American Asthma Foundation and American Lung Association (11-0321) to R. Tsien.

DISCLOSURES

M. Whitney and R. Tsien are scientific advisors to Avelas Biosciences, which has licensed the ACPP technology from the University of California Regents. No other conflicts of interest, financial or otherwise, are declared by the authors.

AUTHOR CONTRIBUTIONS

Author contributions: C.N.F., E.N.S., M.A.W., and R.Y.T. conception and design of research; C.N.F. and E.N.S. performed experiments; C.N.F., E.N.S., and M.A.W. analyzed data; C.N.F., E.N.S., M.A.W., and R.Y.T. interpreted results of experiments; C.N.F. prepared figures; C.N.F. drafted manuscript;

C.N.F., E.N.S., M.A.W., and R.Y.T. edited and revised manuscript; C.N.F., E.N.S., M.A.W., and R.Y.T. approved final version of manuscript.

REFERENCES

- Agrawal DK, Shao Z. Pathogenesis of allergic airway inflammation. *Curr Allergy Asthma Rep* 10: 39–48, 2010.
- Aguilera TA, Olson ES, Timmers MM, Jiang T, Tsien RY. Systemic in vivo distribution of activatable cell penetrating peptides is superior to that of cell penetrating peptides. *Integr Biol (Camb)* 1: 371–381, 2009.
- Antonov AS, Antonova GN, Munn DH, Mivechi N, Lucas R, Catravas JD, Verin AD. AlphaVbeta3 integrin regulates macrophage inflammatory responses via PI3 kinase/Akt-dependent NF-kappaB activation. *J Cell Physiol* 226: 469–476, 2011.
- Barnes PJ. Immunology of asthma and chronic obstructive pulmonary disease. *Nat Rev Immunol* 8: 183–192, 2008.
- Braman SS. The global burden of asthma. *Chest* 130: 4S–12S, 2006.
- Broide DH. Immunologic and inflammatory mechanisms that drive asthma progression to remodeling. *J Allergy Clin Immunol* 121: 560–570; quiz 571–562, 2008.
- Brooks PC, Stromblad S, Sanders LC, von Schalscha TL, Aimes RT, Stetler-Stevenson WG, Quigley JP, Cheresch DA. Localization of matrix metalloproteinase MMP-2 to the surface of invasive cells by interaction with integrin alpha v beta 3. *Cell* 85: 683–693, 1996.
- Cataldo D, Munaut C, Noel A, Franken F, Bartsch P, Foidart JM, Louis R. MMP-2- and MMP-9-linked gelatinolytic activity in the sputum from patients with asthma and chronic obstructive pulmonary disease. *Int Arch Allergy Immunol* 123: 259–267, 2000.
- Cataldo DD, Tournoy KG, Vermaelen K, Munaut C, Foidart JM, Louis R, Noel A, Pauwels RA. Matrix metalloproteinase-9 deficiency impairs cellular infiltration and bronchial hyperresponsiveness during allergen-induced airway inflammation. *Am J Pathol* 161: 491–498, 2002.
- Chen B, Friedman B, Whitney MA, Winkle JA, Lei IF, Olson ES, Cheng Q, Pereira B, Zhao L, Tsien RY, Lyden PD. Thrombin activity associated with neuronal damage during acute focal ischemia. *J Neurosci* 32: 7622–7631, 2012.
- Corry DB, Kiss A, Song LZ, Song L, Xu J, Lee SH, Werb Z, Kheradmand F. Overlapping and independent contributions of MMP2 and MMP9 to lung allergic inflammatory cell egression through decreased CC chemokines. *FASEB J* 18: 995–997, 2004.
- Corry DB, Rishi K, Kanellis J, Kiss A, Song Lz LZ, Xu J, Feng L, Werb Z, Kheradmand F. Decreased allergic lung inflammatory cell egression and increased susceptibility to asphyxiation in MMP2-deficiency. *Nat Immunol* 3: 347–353, 2002.
- Cortez-Retamozo V, Swirski FK, Waterman P, Yuan H, Figueiredo JL, Newton AP, Upadhyay R, Vinegoni C, Kohler R, Blois J, Smith A, Nahrendorf M, Josephson L, Weissleder R, Pittet MJ. Real-time assessment of inflammation and treatment response in a mouse model of allergic airway inflammation. *J Clin Invest* 118: 4058–4066, 2008.
- Cundall M, Sun Y, Miranda C, Trudeau JB, Barnes S, Wenzel SE. Neutrophil-derived matrix metalloproteinase-9 is increased in severe asthma and poorly inhibited by glucocorticoids. *J Allergy Clin Immunol* 112: 1064–1071, 2003.
- Demedts IK, Brusselle GG, Bracke KR, Vermaelen KY, Pauwels RA. Matrix metalloproteinases in asthma and COPD. *Curr Opin Pharmacol* 5: 257–263, 2005.
- Doherty TA, Soroosh P, Broide DH, Croft M. CD4+ cells are required for chronic eosinophilic lung inflammation but not airway remodeling. *Am J Physiol Lung Cell Mol Physiol* 296: L229–L235, 2009.
- Fahy JV, Kim KW, Liu J, Boushey HA. Prominent neutrophilic inflammation in sputum from subjects with asthma exacerbation. *J Allergy Clin Immunol* 95: 843–852, 1995.
- Foley SC, Hamid Q. Images in allergy and immunology: neutrophils in asthma. *J Allergy Clin Immunol* 119: 1282–1286, 2007.
- Gabazza EC, Taguchi O, Tamaki S, Takeya H, Kobayashi H, Yasui H, Kobayashi T, Hataji O, Urano H, Zhou H, Suzuki K, Adachi Y. Thrombin in the airways of asthmatic patients. *Lung* 177: 253–262, 1999.
- Greenlee KJ, Corry DB, Engler DA, Matsunami RK, Tessier P, Cook RG, Werb Z, Kheradmand F. Proteomic identification of in vivo substrates for matrix metalloproteinases 2 and 9 reveals a mechanism for resolution of inflammation. *J Immunol* 177: 7312–7321, 2006.
- Greenlee KJ, Werb Z, Kheradmand F. Matrix metalloproteinases in lung: multiple, multifarious, and multifaceted. *Physiol Rev* 87: 69–98, 2007.
- Holgate ST. Pathogenesis of asthma. *Clin Exp Allergy* 38: 872–897, 2008.
- James AL, Maxwell PS, Pearce-Pinto G, Elliot JG, Carroll NG. The relationship of reticular basement membrane thickness to airway wall remodeling in asthma. *Am J Respir Crit Care Med* 166: 1590–1595, 2002.
- Jiang T, Olson ES, Nguyen QT, Roy M, Jennings PA, Tsien RY. Tumor imaging by means of proteolytic activation of cell-penetrating peptides. *Proc Natl Acad Sci USA* 101: 17867–17872, 2004.
- Kelly EA, Busse WW, Jarjour NN. Increased matrix metalloproteinase-9 in the airway after allergen challenge. *Am J Respir Crit Care Med* 162: 1157–1161, 2000.
- Kim DY, Ryu SY, Lim JE, Lee YS, Ro JY. Anti-inflammatory mechanism of simvastatin in mouse allergic asthma model. *Eur J Pharmacol* 557: 76–86, 2007.
- Kumagai K, Ohno I, Okada S, Ohkawara Y, Suzuki K, Shinya T, Nagase H, Iwata K, Shirato K. Inhibition of matrix metalloproteinases prevents allergen-induced airway inflammation in a murine model of asthma. *J Immunol* 162: 4212–4219, 1999.
- Laitinen A, Altraja A, Kampe M, Linden M, Virtanen I, Laitinen LA. Tenascin is increased in airway basement membrane of asthmatics and decreased by an inhaled steroid. *Am J Respir Crit Care Med* 156: 951–958, 1997.
- Lee SR, Tsuji K, Lee SR, Lo EH. Role of matrix metalloproteinases in delayed neuronal damage after transient global cerebral ischemia. *J Neurosci* 24: 671–678, 2004.
- Lim DH, Cho JY, Miller M, McElwain K, McElwain S, Broide DH. Reduced peribronchial fibrosis in allergen-challenged MMP-9-deficient mice. *Am J Physiol Lung Cell Mol Physiol* 291: L265–L271, 2006.
- Lombard C, Saulnier J, Wallach J. Assays of matrix metalloproteinases (MMPs) activities: a review. *Biochimie* 87: 265–272, 2005.
- Marchica CL, Pinelli V, Borges M, Zimmer J, Narayanan V, Iozzo R, Ludwig MS. A role for decorin in a murine model of allergen-induced asthma. *Am J Physiol Lung Cell Mol Physiol* 300: L863–L873, 2011.
- McMillan SJ, Kearley J, Campbell JD, Zhu XW, Larbi KY, Shipley JM, Senior RM, Nourshargh S, Lloyd CM. Matrix metalloproteinase-9 deficiency results in enhanced allergen-induced airway inflammation. *J Immunol* 172: 2586–2594, 2004.
- Montesirin J, Bonilla I, Camacho MJ, Chacon P, Vega A, Chaparro A, Conde J, Sobrino F. Specific allergens enhance elastase release in stimulated neutrophils from asthmatic patients. *Int Arch Allergy Immunol* 131: 174–181, 2003.
- Nguyen QT, Olson ES, Aguilera TA, Jiang T, Scadeng M, Ellies LG, Tsien RY. Surgery with molecular fluorescence imaging using activatable cell-penetrating peptides decreases residual cancer and improves survival. *Proc Natl Acad Sci USA* 107: 4317–4322, 2010.
- Olson ES, Aguilera TA, Jiang T, Ellies LG, Nguyen QT, Wong EH, Gross LA, Tsien RY. In vivo characterization of activatable cell penetrating peptides for targeting protease activity in cancer. *Integr Biol (Camb)* 1: 382–393, 2009.
- Olson ES, Jiang T, Aguilera TA, Nguyen QT, Ellies LG, Scadeng M, Tsien RY. Activatable cell penetrating peptides linked to nanoparticles as dual probes for in vivo fluorescence and MR imaging of proteases. *Proc Natl Acad Sci USA* 107: 4311–4316, 2010.
- Olson ES, Whitney MA, Friedman B, Aguilera TA, Crisp JL, Baik FM, Jiang T, Baird SM, Tsimikas S, Tsien RY, Nguyen QT. In vivo fluorescence imaging of atherosclerotic plaques with activatable cell-penetrating peptides targeting thrombin activity. *Integr Biol (Camb)* 4: 595–605, 2012.
- Reinhardt AK, Bottoms SE, Laurent GJ, McNulty RJ. Quantification of collagen and proteoglycan deposition in a murine model of airway remodelling. *Respir Res* 6: 30, 2005.
- Roche WR, Beasley R, Williams JH, Holgate ST. Subepithelial fibrosis in the bronchi of asthmatics. *Lancet* 1: 520–524, 1989.
- Savariar EN, Felsen CN, Nashi N, Jiang T, Ellies LG, Steinbach P, Tsien RY, Nguyen QT. Real-time in vivo molecular detection of primary tumors and metastases with ratiometric activatable cell-penetrating peptides. *Cancer Res* 73: 855–864, 2013.
- Schwingshackl A, Duszyk M, Brown N, Moqbel R. Human eosinophils release matrix metalloproteinase-9 on stimulation with TNF-alpha. *J Allergy Clin Immunol* 104: 983–989, 1999.
- Singh B, Fu C, Bhattacharya J. Vascular expression of the alpha(v)beta(3)-integrin in lung and other organs. *Am J Physiol Lung Cell Mol Physiol* 278: L217–L226, 2000.

44. **Stahle-Backdahl M, Parks WC.** 92-kd gelatinase is actively expressed by eosinophils and stored by neutrophils in squamous cell carcinoma. *Am J Pathol* 142: 995–1000, 1993.
45. **Wagers SS, Norton RJ, Rinaldi LM, Bates JH, Sobel BE, Irvin CG.** Extravascular fibrin, plasminogen activator, plasminogen activator inhibitors, and airway hyperresponsiveness. *J Clin Invest* 114: 104–111, 2004.
46. **Whitney M, Crisp JL, Olson ES, Aguilera TA, Gross LA, Ellies LG, Tsien RY.** Parallel in vivo and in vitro selection using phage display identifies protease-dependent tumor-targeting peptides. *J Biol Chem* 285: 22532–22541, 2010.
47. **Whitney M, Savariar EN, Friedman B, Levin RA, Crisp JL, Glasgow HL, Lefkowitz R, Adams SR, Steinbach P, Nashi N, Nguyen QT, Tsien RY.** Ratiometric activatable cell-penetrating peptides provide rapid in vivo readout of thrombin activation. *Angew Chem Int Ed Engl* 52: 325–330, 2013.

